FERGUSON, G., KAITNER, B., CONNETT, B. E. & RENDLE, D. F. (1986). 10th Eur. Crystallogr. Meet. Collect. Abstr., Wroclaw, Poland, Paper 2B–61, p. 204.
GABE, E. J., LE PAGE, Y., CHARLAND, J.-P., LEE, F. L. & WHITE, P. S. (1989). *J. Appl. Cryst.* **22**, 384–387.
HOUGH, E., NEIDLE, S., ROGERS, D. & TROUGHTON, P. G. H. (1973). *Acta Cryst.* B**29**, 365–367.
JOHNSON, C. K. (1976). *ORTEP*II. Report ORNL-5138. Oak Ridge National Laboratory, Tennessee, USA.
MAIN, P., FISKE, S. J., HULL, S. E., LESSINGER, L., GERMAIN, G., DECLERCQ, J.-P. & WOOLFSON, M. M. (1982). *MULTAN*82. *A System of Computer Programs for the Automatic Solution of Crystal Structures from X-ray Diffraction Data.* Univs. of York, England, and Louvain, Belgium.
RENDLE, D. F. & CONNETT, B. E. (1988). *J. Forensic Sci. Soc.* **28**, 295–297.
RENDLE, D. F., GLAZIER, E. J., FERGUSON, G. & JENNINGS, M. C. (1989). Unpublished work.

Acta Cryst. (1991). B**47**, 484–492

Absolute Optical Chirality of Dirubidium (+)-Tartrate and Dicaesium (+)-Tartrate Crystals

BY K. STADNICKA AND Z. BROŻEK

Faculty of Chemistry, Jagiellonian University, ul. Karasia 3, 30-060 *Kraków, Poland*

(*Received* 25 *June* 1990; *accepted* 8 *January* 1991)

Abstract

The crystal structures and absolute optical chiralities of $Rb_2[(2R,3R)\text{-}C_4H_4O_6]$, RBT ($M_r = 319{\cdot}01$) and $Cs_2[(2R,3R)\text{-}C_4H_4O_6]$, CST ($M_r = 413{\cdot}88$) have been determined. For crystals grown from aqueous solutions containing (+)-tartrate ions the specific rotation was observed to be laevo over the visible-wavelength range along the optic axis and the space group was found to be $P3_221$ (D_3^6) in both cases. Crystal data at 298 K, Cu $K\alpha$, $\lambda = 1{\cdot}54178$ Å; for RBT: $a = 7{\cdot}168$ (1), $c = 13{\cdot}097$ (1) Å, $V = 582{\cdot}8$ (2) Å^3, $Z = 3$, $D_x = 2{\cdot}726$, $D_m = 2{\cdot}727$ (3) Mg m^{-3}, $\mu = 16{\cdot}61$ mm^{-1}, $F(000) = 450$, final $R = 0{\cdot}0281$ and $wR = 0{\cdot}0572$ for 804 unique observed reflections; for CST: $a = 7{\cdot}432$ (2), $c = 13{\cdot}526$ (3) Å, $V = 647{\cdot}0$ (5) Å^3, $Z = 3$, $D_x = 3{\cdot}187$ Mg m^{-3}, $\mu = 67{\cdot}56$ mm^{-1}, $F(000) = 558$, final $R = 0{\cdot}0348$ and $wR = 0{\cdot}0521$ for 837 unique observed reflections. The relationship between optical rotation and structural chirality has been traced by following the rules established earlier for inorganic ionic crystals. It is shown that in the reported structures the intermolecular helical atomic arrangement of highly polarizable atoms (mainly oxygens and cations) rather than the contribution from the individual optically active organic molecules is responsible for optical rotation of the crystals. Special attention is paid to possible hydrogen bonds, both inter- and intramolecular, as they significantly influence the shape of the helices. The refractive indices and rotatory power, calculated from the structural data using a point-dipole polarizability theory, agree with the experimental results and support this point of view. Evidence is found that in concentrated solution RBT molecules also form helical arrangements.

Introduction

As was shown by Glazer & Stadnicka (1986) the sense and even the magnitude of optical rotatory power can be explained for almost all the inorganic crystals with known absolute structure, as determined by anomalous X-ray scattering and measurements of the optical rotatory dispersion (ORD) carried out on the same crystal. This was demonstrated for low- and high-quartz, berlinite (α-$AlPO_4$), cinnabar (α-HgS), dicalcium strontium and dicalcium lead propionates, $Bi_{12}SiO_{20}$ and $Bi_{12}GeO_{20}$, and $NaClO_3$ and $NaBrO_3$ as well as α-$LiIO_3$ (see also Stadnicka, Glazer & Moxon, 1985). An effort was made to explain the 'structural part' of the optical rotatory dispersion for α-$NiSO_4.6H_2O$, which is well known for the anomalous behaviour of its ORD (Stadnicka, Glazer & Koralewski, 1987), and also for $ZnSeO_4.6H_2O$ (Stadnicka, Glazer & Koralewski, 1988), which is isostructural to the former and yet shows no *d–d* transitions in the cation. This approach also proved successful for $Bi_{12}TiO_{20}$ (Swindells & Leal Gonzalez, 1988), for paratellurite (α-TeO_2, Thomas, 1988) and for $Ba(NO_2)_2.H_2O$ (Thomas & Gomes, 1989). In each of these materials (isotropic or uniaxial crystals) the sign of optical rotation was found to be correlated with particular helical features in the structure. Recently the approach has been extended to biaxial inorganic crystals (α-HIO_3, Stadnicka & Koralewski, 1991).

The results presented here concern uniaxial crystals of dirubidium (+)-tartrate and dicaesium (+)-tartrate containing chiral optically active organic molecules. These crystals were selected first because they display optical activity along the optic axis with the opposite sign to that observed for their aqueous

0108-7681/91/040484-09$03.00

solutions (Traube, 1895). For both crystals measurement of the dispersion of the refractive indices at room temperature was carried out by Bohatý (1982) who also determined the linear electrooptical tensor $[r_{ijk}]$ and the linear electrostriction tensor $[d_{ijk}]$ for $\lambda = 632{\cdot}8$ nm at 295 K. Although the crystal structure of RBT was published by Bohatý & Fröhlich (1983), H-atom positions were not found and there was no attempt to establish the relationship between the structure and optical activity. Moreover, the structural parameters of RBT were not sufficiently precise for CST optical-activity calculations using the program of Devarajan & Glazer (1986). Thus we were forced to redo the structure determination of RBT and determine the CST structural parameters in relation to the measured optical rotation in each case using the same crystal for both the X-ray and optical study.

Crystal preparation and optical measurements

RBT and CST crystals were obtained from chemical reaction of the appropriate carbonates and (+)-tartaric acid [Rb_2CO_3, 99%, Aldrich Chemical Company Inc.; $Cs_2CO_3.H_2O$, 99%, Koch-Light Ltd; (+)-tartaric acid, c.p., Polskie Odczynniki Chemiczne], and recrystallized from aqueous solutions by slow evaporation at room temperature. Colourless crystals of good optical quality displayed a habit similar to that reported by Traube (1895). Faces: $t\{102\}$, $r\{101\}$, $m\{100\}$, $\tau\{10\bar{2}\}$ and $\rho\{10\bar{1}\}$ were observed for both RBT and CST crystals although, as pointed out by Traube, the rhombohedra were better developed in RBT crystals than in CST, in which the hexagonal prism was the dominant form. The sign of the optical activity was checked for an RBT plate, cut perpendicularly to the optic axis, by rotation of the microscope analyzer and by observation of Airy's spiral. It was found to be negative (laevorotatory crystal) in the visible range of wavelengths. Precise measurements of optical rotation were carried out perpendicular to the c axis using Ar-ion and He/Ne lasers on a 2·48 mm slice cut from the RBT crystal. Unfortunately the CST crystal was highly hygroscopic and we were able to make only one measurement of its optical rotation, at $\lambda = 632{\cdot}8$ nm, because of rapid deterioration of the surface. Both crystals were found to be laevorotatory. The specific rotation of RBT along the optic axis at $\lambda = 457{\cdot}9$, 496·5, 514·5 and 632·8 nm was determined to be $-17{\cdot}8$ (2), $-15{\cdot}75$ (13), $-13{\cdot}75$ (14) and $-8{\cdot}65$ (8)° mm^{-1}, respectively. The measurements are in good agreement with the values calculated from the Drude-type equation, published by Alikhanova, Burkov, Kizel, Klimova, Perekalina, Semin & Chelcov (1977), Fig. 1(*a*). These authors fitted their experimental data, in the range $\lambda = 0{\cdot}200$–$0{\cdot}900$ μm, to equations of both the Drude and Chandrasekhar types. They obtained better agreement for the Drude equation in the case of RBT and for the Chandrasekhar equation in the case of CST. For the CST crystal, a slice of about 2·30 mm in thickness, the observed ρ value was $-9{\cdot}67$ (9)° mm^{-1} while from their equation, $\rho = A_1\lambda^2(\lambda^2 - \lambda_{01}^2)^{-2}$ with $A_1 = -3{\cdot}640$° mm^{-1} μm^2 and $\lambda_{01} = 0{\cdot}150$ μm, it was

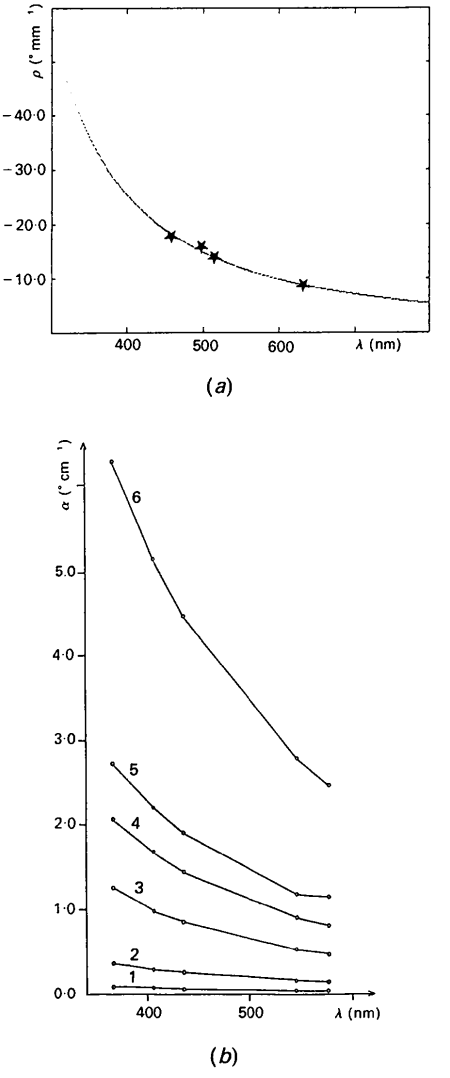

Fig. 1. (*a*) Dispersion of optical rotatory power for the laevorotatory RBT crystal along the optic axis direction. The curve is drawn according to the equation of Alikhanova, Burkov, Kizel, Klimova, Perekalina, Semin & Chelcov, (1977): $\rho = A_1(\lambda^2 - \lambda_{01}^2)^{-1}$ with $A_1 = -3{\cdot}201$° mm^{-1} μm^2 and $\lambda_{01} = 0{\cdot}185$ μm. Our results: $-17{\cdot}8$ (2), $-15{\cdot}75$ (13), $-13{\cdot}75$ (14)° mm^{-1} (Ar laser) and $-8{\cdot}65$ (8)° mm^{-1} (He/Ne laser) are marked by stars. (*b*) Optical rotation of RBT aqueous solutions obtained from the laevorotatory crystal. Range of λ: 366–578 μm, $T = 296$ K, maximal error of $\alpha = 0{\cdot}07$° cm^{-1}. Solution concentrations were: (1) 1·6, (2) 8·0, (3) 30·0, (4) 40·0, (5) 60·0, (3) 120·0 g salt per 100 cm^3 solution. Note that all these solutions are dextrorotatory.

Table 1. *Summary of data collection and structure refinement*

	$Rb_2[(2R,3R)\text{-}C_4H_4O_6]$, $P3_221$ (RBT)	$Cs_2[(2R,3R)\text{-}C_4H_4O_6]$, $P3_221$ (CST)
Optical rotation along c	Laevorotatory	Laevorotatory
Crystal shape and size (mm)	Sphere, $\phi = 0.20$ (1)	Sphere, $\phi = 0.25$ (1) (glass capillary)
Measured D_m	Flotation (toluene and bromoform)	-
Diffractometer	Enraf–Nonius CAD-4 (graphite-monochromated Cu $K\alpha$ radiation)	Enraf–Nonius CAD-4 (graphite-monochromated Cu $K\alpha$ radiation)
Lattice-parameter measurement		
θ range (°), No. of reflections	$6 < \theta < 60$, 25	$6 < \theta < 60$, 25
Intensity measurement		
θ range (°)	$1 \le \theta \le 78$	$1 \le \theta \le 77$
Indices range	$0 \le h \le 9$, $-9 \le k \le 9$, $0 \le l \le 16$	$-9 \le h \le 9$, $-9 \le k \le 0$, $0 \le l \le 17$
Scan width (°) and mode	$0.65 + 0.35\tan\theta$, $\omega/2\theta$	$0.50 + 0.30\tan\theta$, $\omega/2\theta$
Intensity control reflections	006, $1\bar{2}3$ measured every hour	$0\bar{1}3$, $\bar{1}13$ measured every hour
Changes in intensity	< 3.0%	< 9.3%
No. of reflections measured	1441	1416
Criterion for observed reflections	$\lvert F_o\rvert \ge 3\sigma(F_o)$	$\lvert F_o\rvert \ge 4\sigma(F_o)$
No. of observed unique reflections including Friedel opposites, R_{int}	804, 0.025	837, 0.041
Corrections applied	Lorentz, polarization and absorption ($\mu R = 1.66$) effects	Lorentz, polarization and absorption ($\mu R = 8.44$) effects
Max., min. transmission factors	0.2083, 0.1074	0.0410, 0.0019
Extinction reflections omitted	$\bar{2}22$, 031	-
Refinement method	Full-matrix least squares on $\lvert F_o\rvert$	Full-matrix least squares on $\lvert F_o\rvert$
No. of parameters refined	63	62
Non-H atoms	Positional and anisotropic thermal	Positional and anisotropic thermal
H atoms*	Positional and isotropic thermal	Positional and isotropic thermal
Extinction parameter (*SHELX76*)	0.0477 (8)	-
Weighting scheme	$w = k[\sigma^2(F_o) + g(F_o)^2]^{-1}$	$w = k[\sigma^2(F_o) + (F_o)^2]^{-1}$
k and g converged to	1.000, 0.001097	0.2687, 0.000831
R, wR, S	0.0281, 0.0572, 1.5993	0.0348, 0.0521, 0.7989
Average, max. Δ/σ		
Non-H atoms	0.02, 0.10	0.02, 0.07
H atoms	0.03, 0.10	0.04, 0.10
Max., min. height in final difference Fourier map (e Å^{-3})	0.33, −0.29	0.47, −1.09
For antistructure	$Rb_2[(2S,3S)\text{-}C_4H_4O_6]$, $P3_121$ ($\bar{x}\bar{y}\bar{z}$)	$Cs_2[(2S,3S)\text{-}C_4H_4O_6]$, $P3_121$ ($\bar{x}\bar{y}\bar{z}$)
R, wR	0.0349, 0.0708	0.0544, 0.0864

* Initial positional H-atom parameters from the difference Fourier map.

found to be $-10.20°\ mm^{-1}$. As our results are close to theirs we can assume that the optical rotatory dispersion is normal and therefore ρ does not change sign at longer wavelengths. From these laevorotatory crystals spheres suitable for the X-ray experiments were ground. The rest of the large RBT crystal was dissolved in distilled water and the optical rotation of the solution was then measured with a Polamat-A spectropolarimeter (Carl Zeiss Jena) for a few concentrations. The solutions of the laevorotatory crystal were all found to be dextrorotatory over the visible range of wavelengths and optical rotation became more positive with increasing concentration (Fig. 1*b*).

Structure determination

The coordinates of the heavy atoms were found by the super-sharp Patterson procedure of *SHELXS86* (Sheldrick, 1985) and the positions of the O and C atoms were located from subsequent Fourier syntheses. The structure of RBT was essentially the same as that published previously by Bohatý (1982). The data collected for CST were later transformed by the matrix $\bar{1}00/0\bar{1}0/001$ to stress the isomorphism of these two structures. All details of the data collection and structure refinement, performed with the *SHELX76* program (Sheldrick, 1976), are given in Table 1. The weighting scheme applied to both structures effectively suppressed the importance of strong low-angle reflections, for which relatively high errors were proved by analysis of variance at $w = k\sigma^{-2}$, bringing the S factor to reasonable values close to 1.0 at the same time. In the case of CST similar errors were additionally observed for high-angle reflections from the last layer with $k = 9$ in particular as a result of water absorption, which cannot be excluded for such a hygroscopic material, although the crystal was protected by a glass capillary. Because of these errors the value of R_{int} appeared to be slightly higher than the R factor obtained for CST. The difference between R and wR in both compounds could be accounted for in terms of an overestimation of weights for weak reflections. Scattering factors for neutral atoms and anomalous-dispersion corrections were taken from *International Tables for X-ray Crystallography* (1974, Vol. IV). The final atomic coordinates and thermal parameters are listed in Table 2.* Geometric calculations were carried out using the *PARST* program (Nardelli, 1983) and drawings were made by *ORTEP* (Johnson, 1965, 1971). Bond lengths and bond angles as well as cation–oxygen contacts are given in Table 3. The

* A list of structure factors has been deposited with the British Library Document Supply Centre as Supplementary Publication No. SUP 53887 (12 pp.). Copies may be obtained through The Technical Editor, International Union of Crystallography, 5 Abbey Square, Chester CH1 2HU, England.

Table 2. *Fractional coordinates and thermal parameters with e.s.d.'s in parentheses*

U_{ij} ($\times 10^4$) are in Å^2. For H atoms, isotropic U ($\times 10^3$) is given. $T = \exp[-2\pi^2(U_{11}h^2a^{*2} + \ldots + 2U_{12}hka^*b^* + \ldots)]$.

RBT

	x	y	z
Rb	0·53787 (7)	0·20671 (7)	0·05053 (2)
O(11)	0·3302 (4)	0·1862 (4)	0·2493 (2)
O(12)	0·2441 (4)	0·3989 (4)	0·1587 (2)
O(2)	−0·1481 (4)	0·2292 (4)	0·2451 (2)
C(1)	0·2085 (5)	0·2569 (5)	0·2243 (2)
C(2)	−0·0146 (5)	0·1450 (5)	0·2761 (2)
H(O2)	−0·063 (1)	0·361 (1)	0·223 (1)
H(C2)	−0·077 (1)	0·003 (1)	0·256 (1)

	U_{11}	U_{22}	U_{33}	U_{23}	U_{13}	U_{12}
Rb	319 (2)	340 (2)	276 (3)	−25 (1)	68 (1)	106 (2)
O(11)	277 (7)	361 (7)	300 (7)	−3 (7)	55 (7)	200 (6)
O(12)	423 (7)	314 (7)	377 (7)	138 (7)	102 (7)	148 (7)
O(2)	372 (7)	451 (7)	406 (8)	194 (7)	68 (7)	270 (6)
C(1)	299 (8)	235 (8)	160 (7)	−8 (7)	74 (7)	100 (7)
C(2)	242 (7)	207 (7)	223 (8)	19 (7)	−44 (7)	109 (6)
H(O2)	52 (1)					
H(C2)	50 (1)					

CST

	x	y	z
Cs	0·5342 (1)	0·2060 (1)	0·04890 (3)
O(11)	0·3189 (7)	0·1894 (8)	0·2485 (4)
O(12)	0·2336 (9)	0·3925 (8)	0·1636 (4)
O(2)	−0·1403 (8)	0·2331 (8)	0·2476 (4)
C(1)	0·1966 (9)	0·2508 (8)	0·2255 (4)
C(2)	−0·0148 (9)	0·1513 (8)	0·2765 (4)
H(O2)	−0·053 (2)	0·354 (2)	0·220 (2)
H(C2)	−0·081 (2)	−0·006 (2)	0·267 (2)

	U_{11}	U_{22}	U_{33}	U_{23}	U_{13}	U_{12}
Cs	371 (2)	371 (2)	286 (2)	−15 (2)	70 (2)	123 (2)
O(11)	321 (12)	420 (13)	403 (13)	−44 (12)	21 (12)	225 (11)
O(12)	552 (13)	392 (13)	366 (13)	179 (12)	104 (13)	186 (12)
O(2)	375 (12)	522 (13)	344 (13)	108 (12)	14 (12)	282 (11)
C(1)	305 (13)	262 (13)	220 (13)	−113 (12)	−2 (12)	127 (12)
C(2)	312 (13)	282 (13)	216 (13)	−11 (12)	0 (12)	144 (11)
H(C2)	47 (2)					
H(O2)	50 (2)					

$[(2R,3R)\text{-}C_4H_4O_6]^{2-}$ anion has a diad axis through the C(2)—C(2)^i bond. The numbering of the atoms, analogous for both salts, and thermal ellipsoids for RBT are shown in Fig. 2(*a*). The environment of the rubidium cation is presented in Fig. 2(*b*). In the first coordination zone, up to 3·16 Å for RBT and 3·27 Å for CST, there are six O atoms. However, to close the space around Rb^+ (Cs^+) cation, two or even three additional neighbours from the second coordination zone should be taken into account (Table 3). A similar environment, with eight neighbours for Rb^+ and nine neighbours for Cs^+, was also claimed for both the rubidium and caesium hydrogen tartrates (Templeton & Templeton, 1978, 1989).

Packing and hydrogen bonding

The packing of the structure is essentially the same as that published by Bohatý & Fröhlich (1983). From the results of our work a bifurcated hydrogen-bonding arrangement is suggested in which the O(2) atom of the hydroxyl group acts as a donor and the carboxyl O(12) atoms, from the same and adjacent molecules, may be considered as acceptors (Table 4).

Table 3. *Important interatomic distances* (Å) *and angles* (°) *with e.s.d.'s in parentheses*

	RBT $[(2R,3R)\text{-}C_4H_4O_6]^{2-}$	CST $[(2R,3R)\text{-}C_4H_4O_6]^{2-}$
O(11)—C(1)	1·252 (5)	1·243 (10)
O(12)—C(1)	1·257 (4)	1·263 (8)
O(2)—C(2)	1·422 (5)	1·400 (10)
C(1)—C(2)	1·542 (4)	1·526 (8)
C(2)—C(2)^i	1·510 (5)	1·550 (8)
O(2)—H(O2)	0·878 (7)	0·886 (12)
C(2)—H(C2)	0·925 (7)	1·021 (12)
O(11)—C(1)—O(12)	127·3 (4)	125·3 (7)
O(11)—C(1)—C(2)	115·2 (3)	118·2 (5)
O(12)—C(1)—C(2)	117·4 (3)	116·5 (6)
O(2)—C(2)—C(1)	113·3 (3)	114·3 (5)
O(2)—C(2)—C(2)^i	110·7 (3)	110·3 (5)
C(1)—C(2)—C(2)^i	109·2 (3)	109·8 (5)
C(2)—O(2)—H(O2)	107·1 (6)	104·5 (1·0)
O(2)—C(2)—H(C2)	109·1 (6)	114·5 (9)
C(1)—C(2)—H(C2)	104·6 (6)	106·8 (9)
C(2)^i—C(2)—H(C2)	109·7 (7)	100·1 (1·2)
Cation environment	Rb^+	Cs^+
O(11)^{ii}	2·848 (3)	2·998 (6)
O(11)^{iii}	2·854 (2)	3·013 (4)
O(11)	2·966 (3)	3·109 (6)
O(12)^{iv}	2·974 (3)	3·103 (6)
O(12)^v	3·043 (3)	3·158 (5)
O(2)^{vi}	3·163 (3)	3·267 (5)
O(2)^{vi}	3·350 (3)	3·554 (6)
O(12)	3·353 (4)	3·523 (7)
O(2)^{viii}	3·504 (4)	3·689 (7)

Symmetry code: (i) $-x+1, -x+y+1, -z+\frac{2}{3}$; (ii) $-y+1, x-y, z-\frac{1}{3}$; (iii) $x-y, -y, -z+\frac{1}{3}$; (iv) $y, x, -z$; (v) $x-y+1, -y+1, -z+\frac{1}{3}$; (vi) $x+1, y, z$; (vii) $-y+1, x-y+1, z-\frac{1}{3}$; (viii) $x-y+1, -y, -z+\frac{1}{3}$.

Thus, one component of the bifurcated hydrogen bond is intermolecular and the second is intramolecular. In the RBT structure the strengths of both hydrogen bonds are comparable and they both deviate significantly from linearity. In the CST structure the intermolecular hydrogen bond seems to be much weaker than the intramolecular one, because the organic molecules are moved apart by larger cations. A similar tendency of the $[(2R,3R)\text{-}C_4H_4O_6]^{2-}$ anions to form a bifurcated hydrogen bond is also found in the structure of dipotassium (+)-tartrate hemihydrate (Stadnicka, Olech & Koralewski, 1991). Such a bifurcated hydrogen bond is possible as the number of expected acceptors exceeds the number of potential donors in the crystal structure and it should influence the conformation of the molecule of a certain configuration. A comparison, based on torsional angles, of the conformations found for the (2*R*,3*R*)-tartrate anion in different crystal environments is given in Table 5. Firstly, the presence of hydrogen in the carboxyl group significantly affects the O(12)C(1)C(2)O(2) and O(12)C(1)C(2)C(2)^i angles, which are about 10 and −112°, respectively, while for the deprotonated carboxyl group they are changed to approximately 0 and −126°. The torsion angles of the H(O2)O(2)C(2)C(1) type are close to 0° (−14° on average), in contrast to the much higher values usually observed, and could account for the intra-

molecular interaction between the H atom of the hydroxyl group acting as a donor and an adjacent carboxylic oxygen acting as an acceptor. Moreover, in (+)-tartaric acid itself an intramolecular hydrogen bond may be expected between two hydroxyl groups. This is supported by the O(2)C(2)C(2)^{i}O(2)^{i} torsion angle decreasing from -70 to $-58°$. From the results of its structure analysis (Hope & de la Camp, 1972) a trifurcated hydrogen bond, with two inter- and one intramolecular components, cannot be excluded (Table 4).

In conclusion, the non-linearity of the hydrogen bonding observed in the RBT and CST structures, and also in some other tartrates, is consistent with the Finney & Savage (1988) approach in that the electrostatics do not dominate the directionality of hydrogen bonding and the anisotropy of repulsion should also be taken into account as an essential part of the description.

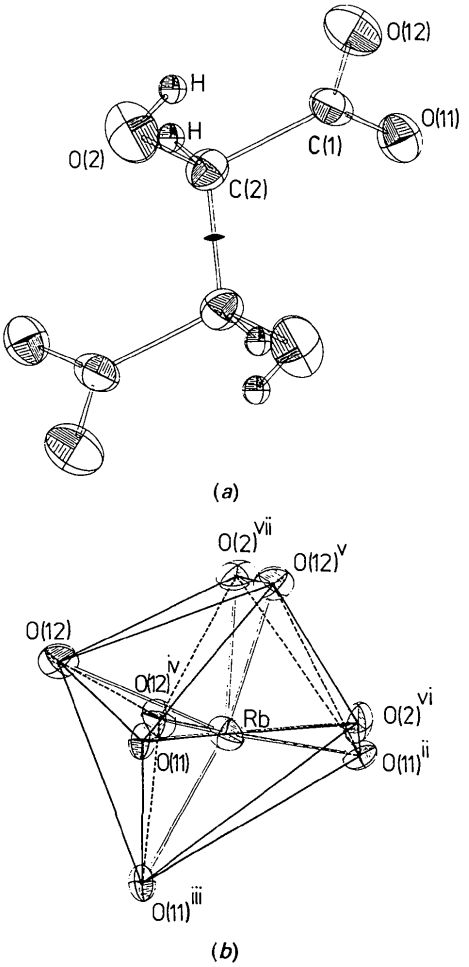

Fig. 2. (*a*) RBT: projection of the $[(2R,3R)\text{-}C_4H_4O_6]^{2-}$ anion along the twofold axis. The atom numbering is shown. Thermal-vibration ellipsoids are scaled to enclose 50% probability. (*b*) RBT: cation environment projected on (001). O(2)^{vi} and O(12) but not O(2)^{viii} (Table 3) are necessary to fill the space around the Rb cation.

Discussion

To explain the optical activity of the RBT and CST crystals, a simple visual approach according to the rules worked out by Glazer & Stadnicka (1986) for inorganic crystals was used, and detailed calculations of the magnitude and sense of optical rotation were made using the program of Devarajan & Glazer (1986).

(*a*) Taking Pauling's (1927) molar refraction values as a guideline to estimate electronic polarizability volumes for O^{2-} 3·92, Rb^{+} 1·42, and Cs^{+} 2·44 Å^3, to be compared with C^{4+} 0·001 Å^3, it is clear that only O atoms and possibly the cations should be considered to be sufficiently polarizable.

(*b*) Considering the shortest contacts between the O atoms (up to 3·3 Å) one can trace three interpenetrating non-symmetric structural helices (Fig. 3*a*) parallel to [001], related by the 3_2 screw axis. Each of these helices has twofold symmetry perpendicular to the helix axis and repeats every *c* distance. Such a single helix is right-handed, *i.e.*, it turns to the right away from the observer, and so it has a chirality opposite to that of the 3_2 screw axis (Figs. 3*b*,*c*). There are eight oxygens per helix repeat distance *c*, but only three sets of equivalent atoms: carboxyls O(11) and O(12), and hydroxyl O(2). Therefore, the helices can be described as *RS*3/8 according to the notation of Glazer & Stadnicka (1986). Note that the helices along the optic axis direction are very distorted due to the strong hydrogen bonds discussed earlier [see 2·691 (4) and 2·844 (5) Å for RBT in Fig. 3(*c*) or 2·669 (8) and 3·042 (6) Å for CST]. It is not possible to find other atomic helices along [001] with short enough (smaller than 3·5 Å) O—O distances.

(*c*) The anisotropic polarizability volumes represented by ellipsoids are expected to be roughly 'perpendicular' to the thermal ellipsoids of the atoms, *i.e.*, the angles between the largest thermal and polarizability eigenvalues should be close to 90°. On the other hand the strong covalent C—O bonds (Fig. 3*a*) should also influence the directions of the *largest components of the polarizability volumes*. Hence, they would be more or less tangential to the helix causing the incident polarized light to rotate in the same sense as that of the helix, *i.e.*, laevo along the optic axis.

(*d*) It is also interesting to look for helices in the directions perpendicular to the optic axis, especially those with the shortest repeat distances. The possible helices are *LS*2/4 with period *a*, consisting of Rb and O(11); *LS*3/6 (2*a*) consisting of Rb, O(12) and O(2); and *RS* 2/4 (*a*) consisting of O(12) and O(2) (Fig. 4).

Table 4. *Geometry of the hydrogen bonding in the* RBT *and* CST *crystal structures together with similar features of some hydrogen bonds in the other tartrates (structural data taken from publications quoted at the foot of Table 5)*

D—H···*A*	*A*(coordinates)	*D*···*A* (Å)	*D*—H (Å)	H···*A* (Å)	*DHA* (°)
CST					
O(2)—H···O(12)	x, y, z	2·67 (1)	0·89 (2)	2·15 (2)	117 (1)
O(2)—H···O(12)	$x-y, -y+1, -z+\frac{1}{3}$	3·04 (1)	0·89 (2)	2·47 (2)	123 (1)
O(2)H···O(2)H	$-x+1, -x+y+1, -z+\frac{2}{3}$	2·94 (1)*			
RBT					
O(2)—H···O(12)	x, y, z	2·691 (4)	0·88 (1)	2·24 (1)	112 (1)
O(2)—H···O(12)	$x-y, -y+1, -z+\frac{1}{3}$	2·844 (4)	0·88 (1)	2·22 (1)	127 (1)
O(2)H···O(2)H	$-x+1, -x+y+1, -z+\frac{2}{3}$	2·954 (4)*			
DKT					
O(3)—H···O(41)	x, y, z	2·667 (2)	0·89 (1)	2·30 (1)	105 (1)
O(3)—H···O(42)	$-x+\frac{3}{2}, y+\frac{1}{2}, -z+\frac{3}{2}$	2·846 (2)	0·89 (1)	2·03 (1)	153 (1)
O(3)H···O(2)H	x, y, z	2·881 (2)*			
KHT					
O(4)—H···O(6)	x, y, z	2·694 (2)	0·83 (3)	2·55 (4)	91 (2)
O(4)—H···O(5)	$x-\frac{1}{2}, -y+\frac{1}{2}, -z$	2·783 (2)	0·83 (3)	1·97 (3)	167 (4)
O(4)H···O(3)H	x, y, z	2·947 (2)*			
DST					
O(3)—H···O(1)	x, y, z	2·60 (4)	0·90 (2)	2·04 (3)	119 (1)
O(3)—H···O(8)H$_2$	x, y, z	2·95 (3)	0·90 (2)	2·53 (3)	109 (1)
O(3)H···O(4)H	x, y, z	2·94 (3)*			
TA					
O(4)—H···O(1)H	x, y, z	2·864 (1)	0·86 (2)	2·55 (2)	103 (2)
O(4)—H···O(3)	$-x+1, y-\frac{1}{2}, -z+1$	2·876 (1)	0·86 (2)	2·09 (3)	152 (2)
O(4)H···O(1)H	$-x+1, y-\frac{1}{2}, -z+1$	3·001 (1)	0·86 (2)	2·50 (2)	118 (2)

* No hydrogen bonding.

Table 5. *Comparison of torsion angles* (°) *and dihedral angles* (°) *between two planes of* O(11)O(12)C(1)C(2)O(2) *for selected ditartrates, hydrogen tartrates and tartaric acid*

	CST	RBT	DKT	CSHT	RBHT	KHT	TA
O(11)—C(1)—C(2)—O(2)	178·7 (6)	−179·7 (3)	180·0 (2)	−169·9 (2)	−170·7 (2)	−171·4 (1)	−177·5 (1)
O(12)—C(1)—C(2)—O(2)	−0·4 (8)	−3·5 (4)	0·6 (3)	10·1 (3)	10·4 (3)	9·5 (2)	5·2 (2)
O(11)—C(1)—C(2)—C(2)^i	54·0 (7)	56·7 (4)	59·9 (2)	69·1 (2)	67·7 (3)	66·6 (2)	62·8 (1)
O(12)—C(1)—C(2)—C(2)^i	−125·0 (6)	−127·1 (3)	−119·5 (2)	−110·9 (2)	−111·3 (3)	−112·6 (2)	−114·6 (1)
H(O2)—O(2)—C(2)—C(1)	−18 (1)	−23 (1)	96 (1)	128 (1)	122 (1)	−58 (1)	164 (1)
C(1)—C(2)—C(2)^i—O(2)^i	56·8 (7)	54·4 (3)	53·5 (2)	51·7 (2)	52·4 (3)	54·4 (2)	59·7 (1)
O(2)—C(2)—C(2)^i—O(2)^i	−70·1 (7)	−70·7 (3)	−69·5 (2)	−69·7 (2)	−69·5 (2)	−68·2 (2)	−58·1 (1)
C(1)—C(2)—C(2)^i—C(1)^i	−176·4 (5)	179·5 (3)	179·1 (2)	178·6 (2)	179·1 (2)	179·7 (1)	175·4 (1)
O(2)—C(2)—C(2)^i—C(1)^i	56·8 (7)	54·4 (3)	56·2 (2)	57·2 (2)	57·3 (2)	57·2 (2)	66·8 (1)
O(11)^i—C(1)^i—C(2)^i—O(2)^i	178·7 (6)	−179·7 (3)	−173·8 (2)	176·0 (2)	178·3 (2)	178·9 (1)	−174·3 (1)
O(12)^i—C(1)^i—C(2)^i—O(2)^i	−0·4 (8)	−3·5 (4)	5·2 (3)	−4·2 (3)	−0·5 (3)	0·9 (2)	4·9 (2)
O(11)^i—C(1)^i—C(2)^i—C(2)	54·1 (7)	56·7 (4)	63·0 (2)	50·4 (3)	52·8 (3)	54·8 (2)	61·0 (2)
O(12)^i—C(1)^i—C(2)^i—C(2)	−125·0 (6)	−127·2 (3)	−118·1 (2)	−129·7 (2)	−126·0 (2)	−123·3 (1)	−119·8 (2)
H(O2)^i—O(2)^i—C(2)^i—C(1)^i	−18 (1)	−23 (1)	10 (1)	−56 (1)	−64 (1)	128 (1)	−72 (1)
Dihedral angle	69·3 (2)	70·2 (1)	59·0 (1)	62·2 (1)	60·0 (1)	59·27 (4)	56·6 (1)

Notes: CST, RBT (this work); DKT, $K_2[(2R,3R)\text{-}C_4H_4O_6].0{\cdot}5H_2O$ (Stadnicka, Olech & Koralewski, 1991); CSHT, $Cs[(+)\text{-}C_4H_5O_6]$ (Templeton & Templeton, 1978); RBHT, $Rb[(+)\text{-}C_4H_5O_6]$ (Templeton & Templeton, 1989); KHT, $K[(+)\text{-}C_4H_5O_6]$ at 100 K (Buschmann & Luger, 1985); TA, $(+)\text{-}C_4H_6O_6$ (Hope & de la Camp, 1972); DST, $Na[(+)\text{-}C_4H_4O_6].H_2O$ (Ambady & Kartha, 1968). For CSHT, RBHT and KHT the carboxylic H atom is at O(11), for TA at O(11) and O(11)^i.

The first helix seems to be the most responsible for optical rotation in this case with an additional contribution from the second helix. For the third helix the polarizability ellipsoid of O(2) seems to be radial whereas that of O(12) is tangential to the helix so that it is difficult to predict its contribution to the resultant optical rotation. In conclusion, the specific rotation of the RBT crystal in the directions perpendicular to the optic axis is expected to be positive (dextrorotatory). This is in agreement with the suggestion of Pine & Dresselhaus (1972) that in uniaxial crystals there should be a simple relationship between $\rho_\parallel$ and $\rho_\perp$, *i.e.*, in directions parallel and perpendicular to the optic axis, respectively: $\rho_\perp \simeq -(a/c)\rho_\parallel$. It is worth mentioning that the measurement of $\rho_\perp$ in the presence of linear birefringence is possible only with recourse to specialized techniques, *e.g.*, Kobayashi & Uesu (1983) and Moxon & Renshaw (1990).

For optical-activity calculations at a given wavelength the input isotropic polarizability volumes (α/Å^3) of the contributing atoms, normalized by the

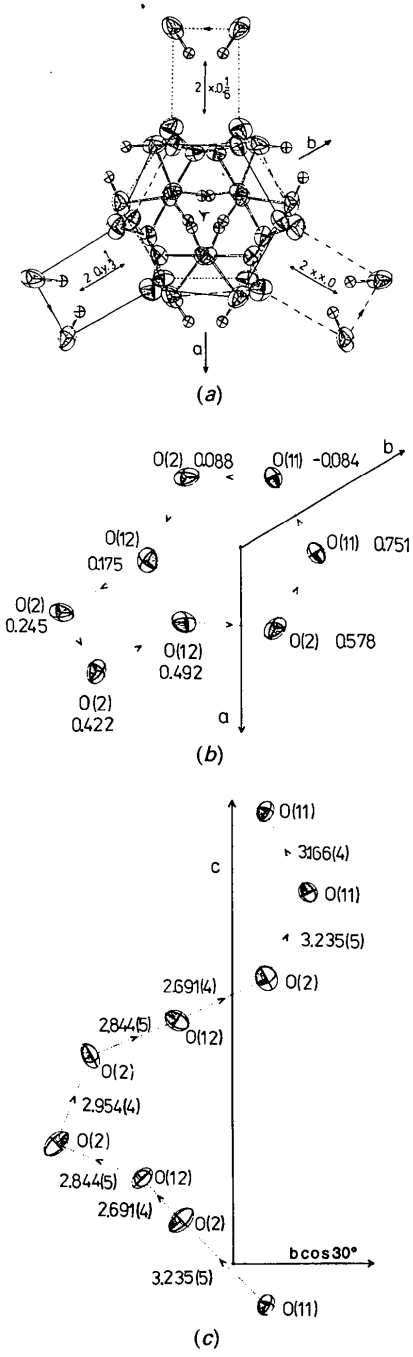

Fig. 3. Intermolecular helices responsible for the optical rotation along the optic axis. O and C atoms are represented by thermal ellipsoids at 50% probability. (*a*) Three helices of the *RS*3/8 type, related by a 3_2 axis, in (001) projection. They are marked by full, broken and dotted lines, respectively. (*b*) Single *RS*3/8 helix projected along [001] with atom heights for RBT in fractions of *c*. For CST the heights are −0·085, 0·086, 0·170, 0·248, 0·419, 0·497, 0·581 and 0·752, respectively. (*c*) The same helix in projection along [100] with the lengths of O···O distances (Å) given for RBT. In CST the corresponding distances, starting from the lowest O(11) atom, are: 3·282 (9), 2·669 (8), 3·042 (6), 2·940 (7), 3·042 (6), 2·669 (8), 3·282 (9) and 3·293 (7) Å, respectively.

Clausius–Mosotti formula, were chosen by trial-and-error to achieve the best agreement between observed and calculated refractive indices. At a given wavelength the input polarizability volumes assumed for individual atoms influenced the variation of the refractive indices (both ordinary, n_o, and extraordinary, n_e) as well as $\rho_\parallel$ and $\rho_\perp$. It was found that for an increase in input α, in the case of Rb (or Cs) and O(2), n_o was reduced and ρ was increased to more positive values. In the case of O(11) and O(12) the opposite influence on n_o was observed, *i.e.*, n_o was increased and ρ decreased to more negative values. Both RBT and CST crystals are optically negative and in order to obtain the proper relationship between n_o and n_e ($n_e < n_o$), the contribution of the C atoms, albeit very small, has to be taken into account. Slightly higher values of input α_C produced an increase in n_o, strongly changed n_e and decreased ρ. Although a very small value of input polarizability volume was attributed to the C atoms, their presence could not be neglected in the calculations as they significantly modified the anisotropy of polarizability volume for highly polarizable O atoms through strong covalent C—O bonds in the tartaric anion. The best input data and the results obtained are given in Table 6. From a comparison of Figs. 3(*b*) and 3(*c*) with Fig. 5 it is clear that the polarizability

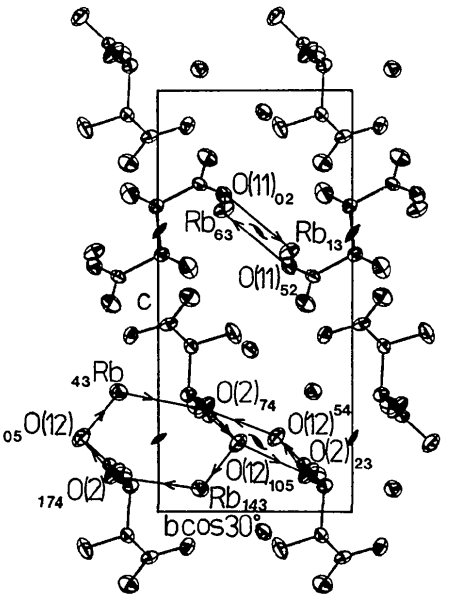

Fig. 4. The possible helices perpendicular to the optic axis in the projection of RBT along [100] (atoms are represented by thermal ellipsoids and their fractional heights are given in hundreds of *a*). *LS*2/4 with the repeat distance *a*, consists of O(11) and Rb atoms [O(11)···Rb = 2·848 (3), Rb···O(11) = 2·854 (2) Å]; double helix *LS*3/6, 2*a*: O(12), Rb and O(2) [O(12)···Rb = 3·353 (4), Rb···O(2) = 3·163 (2) and O(2)···O(12) = 2·691 (4) Å]; *RS*2/4, *a*: O(2) and O(12) [O(2)···O(12) = 2·691 (4) and O(12)···O(2) = 2·844 (5) Å].

Table 6. *Isotropic polarizability volume input data and results obtained from calculations with the program of Devarajan & Glazer* (1986) *for* $\lambda = 632{\cdot}8$ nm

The input values of α are normalized according to the Clausius–Mosotti formula: $\frac{4}{3}\pi\alpha_{uc} = V_{uc}(n^2-1)(n^2+2)^{-1}$, where V_{uc} = unit-cell volume, n = an average refractive index, $\alpha_{uc} = 6(\alpha_{Rb/Cs} + \alpha_{O11} + \alpha_{O12} + \alpha_{O2} + 2\alpha_C)$. For $\sigma(n) = 0{\cdot}001$ and $\sigma(V) = 0{\cdot}5$ Å^3 and assuming that e.s.d.'s of the isotropic polarizability volume for non-equivalent atoms are equal and independent, $\sigma(\alpha_j)$ should be about 0·003. This is a very rough estimation as in the crystal structure α_j depends strongly on the type of atom and its surroundings and thus $\sigma(\alpha_j)$ cannot fulfil the assumptions. It is better therefore to consider how differences in the input data influence the calculated values of refractive indices and optical rotation (compare results for two sets of input data in the case of CST).

	Input α (Å^3)				
	RBT		CST		
Rb (Cs)	1·495		1·782	1·721	
O(11)	1·923		2·235	2·483	
O(12)	1·624		1·782	1·662	
O(2)	1·993		2·235	2·176	
C(1), C(2)	0·007		0·006	0·002	
	Calc.	Obs.	Calc.	Calc.	Obs.
n_o	1·5424	1·5420[a]	1·5665	1·5662	1·5664[a]
n_e	1·5285	1·5298[a]	1·5503	1·5494	1·5495[a]
Δ_n	−0·0139	−0·0122	−0·0162	−0·0168	−0·0169
$\rho_{[001]}$ (° mm^{-1})	−8·53	−8·65[c] −8·74[b]	−12·04	−10·90	−9·67[c] −10·20[b]
$\rho_{[100]}$ (° mm^{-1})	+4·78	+4·73[c,d] +4·78[b,d]	+6·58	+6·88	+5·31[c,d] +5·60[b,d]

Notes: (*a*) Bohatý (1982); (*b*) Alikhanova, Burkov, Kizel, Klimova, Perekalina, Semin & Chelcov (1977); (*c*) our measurements, (*d*) prediction, $\rho_\perp \approx -(a/c)_{\parallel}$.

and thermal ellipsoids of the appropriate atoms tend to be approximately 'perpendicular' to each other as expected. Moreover, despite the differences in isotropic polarizability volume input data for RBT and CST, the orientation of calculated polarizability ellipsoids and their general appearance are very similar in both cases (compare Figs. 5*a* and 5*b*).

Concluding remarks

The absolute chiralities of isomorphous $Rb_2[(2R,3R)\text{-}C_4H_4O_6]$ and $Cs_2[(2R,3R)\text{-}C_4H_4O_6]$ crystals have been established through the determination of the link between their optical activities and structural chiralities. It has been shown that the relationship between optical rotation and absolute crystal structure for organic compounds, even for those containing chiral molecules, can be explained following the rules found for purely inorganic crystals (Glazer & Stadnicka, 1986). In the reported structures, intermolecular helices consisting of highly polarizable atoms were found to be responsible for the sign and the magnitude of optical rotation both along the optic axis (where the sign of optical rotation is opposite to, and its magnitude is very much higher than that found for aqueous solutions of the crystal) and perpendicular to it. Atoms with low polarizability volume cannot be neglected completely, especially when they influence significantly the anisotropy of the polarizability of highly polarizable atoms through strong covalent bonds. For a chosen λ from the long-wavelength range, the values of specific rotation as well as refractive indices calculated from the simple anisotropic polarizability theory (Devarajan & Glazer, 1986) are in good agreement with the observed data. On the other hand, for the RBT crystal the average value of the optical rotation over all directions, $\langle\rho\rangle \simeq +0{\cdot}3°$ mm^{-1} ($\lambda = 632{\cdot}8$ nm), appears to be of the same sign and the same order of magnitude as for a saturated aqueous solution ($\alpha \simeq +0{\cdot}2°$ mm^{-1}) in which the estimated volume per tartrate molecule, assuming the density of such a solution to be 1·801 (1) Mg m^{-3} at room temperature, is only about 2·3 times greater than that in the RBT crystal. It suggests that in concentrated solution the optical rotation is primarily due to intermolecular contacts probably resulting from fluctuating local helical molecular clusters of random orientation rather than from the tartrate species alone. Moreover, for certain tartrates the sign and value of the optical rotation of the solution often depends on the type of solvent. For example, tartaric acid itself shows a specific rotation in aqueous solution of $[\alpha]_D^{20°C} = +14{\cdot}40°$ ($c = 5$ g/100 ml) whereas in 1:1 ethanol and chlorobenzene mixture $[\alpha]_D^{20°C} = -8{\cdot}09°$ (Hallas, 1965). Thus, it supports the idea that the specific rotation of a solution, at least close to saturation, is determined by helical arrangements of both solvent and solvate interacting molecules rather than by the chirality of the solvate molecules alone.

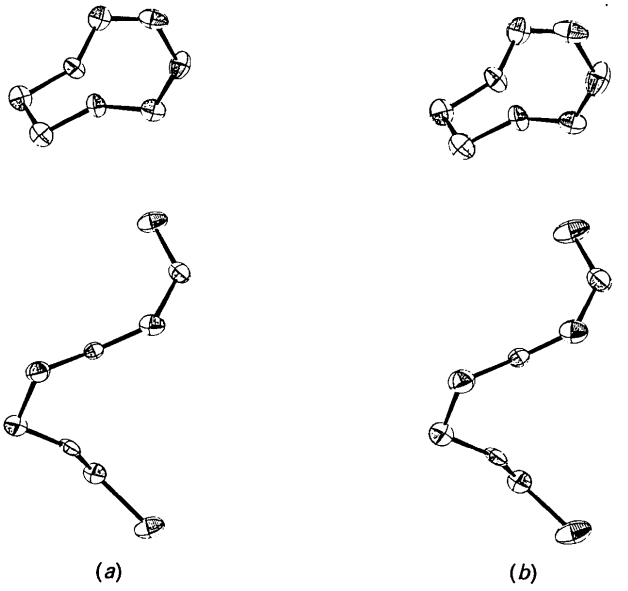

Fig. 5. Single helix *RS*3/8, parallel to the optic axis, projected along both [001] and [100]. O atoms are represented by polarizability ellipsoids (on an arbitrary scale) calculated for the input data given in Table 6. (*a*) RBT (to be compared with Figs. 3*a* and 3*b*). (*b*) CST.

We are grateful to SLAFiBS UJ, Kraków, for making the CAD-4 diffractometer available. We wish to thank Dr A. M. Glazer (Oxford University) for discussions and Dr M. Koralewski for help with the optical measurements. This work was partially supported by the Polish Ministry of Education under project No. RP. II. 10.

References

ALIKHANOVA, Z. M., BURKOV, V. I., KIZEL, V. A., KLIMOVA, A. Y., PEREKALINA, Z. B., SEMIN, G. S. & CHELCOV, P. A. (1977). *Zh. Prikl. Spektrosk.* **27**, 315–321.
AMBADY, G. K. & KARTHA, G. (1968). *Acta Cryst.* B**24**, 1544–1547.
BOHATÝ, L. (1982). *Z. Kristallogr.* **161**, 303–306.
BOHATÝ, L. & FRÖHLICH, R. (1983). *Z. Kristallogr.* **164**, 291–295.
BUSCHMANN, J. & LUGER, P. (1985). *Acta Cryst.* C**41**, 206–208.
DEVARAJAN, V. & GLAZER, A. M. (1986). *Acta Cryst.* A**42**, 560–569.
FINNEY, J. L. & SAVAGE, H. F. J. (1988). *J. Mol. Struct.* **177**, 23–41.
GLAZER, A. M. & STADNICKA, K. (1986). *J. Appl. Cryst.* **19**, 108–122.
HALLAS, G. (1965). *Organic Stereochemistry*. London: McGraw-Hill.
HOPE, H. & DE LA CAMP, U. (1972). *Acta Cryst.* A**28**, 201–207.
JOHNSON, C. K. (1965). *ORTEP*. Report ORNL-3794. Oak Ridge National Laboratory, Tennessee, USA.
JOHNSON, C. K. (1971). *ORTEP*II. Report ORNL-3794, revised. Oak Ridge National Laboratory, Tennessee, USA.
KOBAYASHI, J. & UESU, Y. (1983). *J. Appl. Cryst.* **16**, 204–211.
MOXON, J. R. L. & RENSHAW, A. R. (1990). *J. Phys. Condens. Matter*, **2**, 6807–6836.
NARDELLI, M. (1983). *Comput. Chem.* **7**, 95–98.
PAULING, L. (1927). *Proc. R. Soc. London Ser. A*, **114**, 181–211.
PINE, A. S. & DRESSELHAUS, G. (1972). *Proc. Int. Sch. Phys. Enrico Fermi*, Course LII, *Atomic Structure and Properties of Solids*, edited by E. BURSTEIN. London: Academic Press.
SHELDRICK, G. M. (1976). *SHELX*76. Program for crystal structure determination. Univ. of Cambridge, England.
SHELDRICK, G. M. (1985). *SHELXS*86. *Crystallographic Computing* 3, edited by G. M. SHELDRICK, C. KRÜGER & R. GODDARD, pp. 175–189. Oxford Univ. Press.
STADNICKA, K., GLAZER, A. M. & KORALEWSKI, M. (1987). *Acta Cryst.* B**43**, 319–325.
STADNICKA, K., GLAZER, A. M. & KORALEWSKI, M. (1988). *Acta Cryst.* B**44**, 356–361.
STADNICKA, K., GLAZER, A. M. & MOXON, J. R. L. (1985). *J. Appl. Cryst.* **18**, 237–240.
STADNICKA, K. & KORALEWSKI, M. (1991). In preparation.
STADNICKA, K., OLECH, A. & KORALEWSKI, M. (1991). In preparation.
SWINDELLS, D. C. N. & LEAL GONZALES, J. (1988). *Acta Cryst.* B**44**, 12–15.
TEMPLETON, L. K. & TEMPLETON, D. H. (1978). *Acta Cryst.* A**34**, 368–371.
TEMPLETON, L. K. & TEMPLETON, D. H. (1989). *Acta Cryst.* C**45**, 675–676.
THOMAS, P. A. (1988). *J. Phys. C*, **21**, 4611–4627.
THOMAS, P. A. & GOMES, E. (1989). *Acta Cryst.* B**45**, 348–355.
TRAUBE, H. (1895). *Neues Jahrb. Mineral. Geol.* **10**, 788–800.

Acta Cryst. (1991). B**47**, 492–498

Structure of 14β-Hydroxyprogesterone

BY CONNIE K. CHO AND ANTHONY S. SECCO*

Department of Chemistry, University of Manitoba, Winnipeg, Manitoba, Canada R3T 2N2

(*Received* 20 *August* 1990; *accepted* 2 *January* 1991)

Abstract

14β-Hydroxy-4-pregnene-3,20-dione, $C_{21}H_{30}O_3$, $M_r = 330{\cdot}47$, monoclinic, $P2_1$, $a = 11{\cdot}831\ (3)$, $b = 8{\cdot}096\ (2)$, $c = 18{\cdot}696\ (6)$ Å, $\beta = 91{\cdot}38\ (2)°$, $V = 1790{\cdot}3\ (8)$ Å^3, $Z = 4$, D_m(flotation) = 1·225, $D_x = 1{\cdot}226$ g cm^{-3}, λ(Mo $K\alpha$) = 0·71069 Å, $\mu = 0{\cdot}86$ cm^{-1}, $F(000) = 720$, $T = 294$ K, $R = 0{\cdot}036$ for 1588 reflections with $I \geq 3\sigma(I)$. The structures of both conformers (I) and (II) in the asymmetric unit resemble the typical cardiac glycoside digitoxigenin, with *cis C/D* ring junctions. *B* and *C* rings are in chair conformations. Both *A* rings are between sofa and half-chair conformations, with the 3-carbonyl O atom bent out of the ring plane. The *D* ring of (I) exists primarily as a half-chair stabilized by *intra*-molecular hydrogen bonding between O(14) and O(20), whereas the *D* ring of (II) is a deep envelope stabilized by *inter*molecular hydrogen bonding between O(14) and O(14)′. The C(16)—C(17)—C(20)—O(20) torsion angle is equal to −46·8°, similar to the majority of other progestins, while C(16)′—C(17)′—C(20)′—O(20)′ has an unusual torsion angle of 168·8° which is a probable result of crystal packing forces. The relative spatial displacements of O(20) and O(20)′ from O(4) of digitoxigenin are 2·88 and 2·87 Å, respectively, which are shorter than expected based on receptor affinity.

Introduction

14β-Hydroxyprogesterone is the first semisynthetic analog of hydroxyprogesterone which induces

* To whom all correspondence should be addressed.

0108-7681/91/040492-07$03.00